2021

TRICHOTORQUATUS GEN. NOV. - A NEW GENUS OF SOIL CYANOBACTERIA DISCOVERED FROM AMERICAN DRYLANDS

Nicole Pietrasiak
New Mexico State University

Sharon Reeve
San Diego State University

Karina Osorio-Santos
Universidad Nacional Autonoma de Mexico

David A. Lipson
San Diego State University

Jeffrey R. Johansen
John Carroll University, johansen@jcu.edu

TRICHOTORQUATUS GEN. NOV. - A NEW GENUS OF SOIL CYANOBACTERIA DISCOVERED FROM AMERICAN DRYLANDS[1]

Nicole Pietrasiak[2]

Plant and Environmental Sciences Department, New Mexico State University, 945 College Drive, Las Cruces, New Mexico 88003, USA

Sharon Reeve

Department of Biology, San Diego State University, 5500 Campanile Drive, Mail Code 4614, San Diego, California 92182, USA

Karina Osorio-Santos

Departamento de Biología Comparada, Universidad Nacional Autónoma de México (UNAM), Colonia Coyoacán, Código Postal 04451070474, P.O. Box 70–474, Ciudad de México, México

David A. Lipson

Department of Biology, San Diego State University, 5500 Campanile Drive, Mail Code 4614, San Diego, California 92182, USA

and Jeffrey R. Johansen

Department of Biology, John Carroll University, University Heights, Ohio 44118, USA

Department of Botany, Faculty of Sciences, University of South Bohemia, Branišovská 31, České Budějovice 370 05, Czech Republic

Cyanobacteria are crucial ecosystem components in dryland soils. Advances in describing α–level taxonomy are needed to understand what drives their abundance and distribution. We describe *Trichotorquatus* gen. nov. (Oculatellaceae, Synechococcales, Cyanobacteria) based on four new species isolated from dryland soils including the coastal sage scrub near San Diego, California (USA), the Mojave and Colorado Deserts with sites at Joshua Tree National Park and Mojave National Preserve, California (USA), and the Atacama Desert (Chile). The genus is morphologically characterized by having thin trichomes (<4.5 µm wide), cells both shorter and longer than wide, rarely occurring single and double false branching, necridia appearing singly or in rows, and sheaths with a distinctive collar-like fraying and widening mid-filament, the feature for which the genus is named. The genus is morphologically nearly identical with *Leptolyngbya* sensu stricto but is phylogenetically quite distant from that genus. It is consequently a cryptic genus that will likely be differentiated in future studies based on 16S rRNA sequence data. The type species, *T. maritimus* sp. nov. is morphologically distinct from the other three species, *T. coquimbo* sp. nov., *T. andrei* sp. nov. and *T. ladouxae* sp. nov. However, these latter three species are morphologically very close and are considered by the authors to be cryptic species. All species are separated phylogenetically based on sequence of the 16S-23S ITS region. Three distinct ribosomal operons were recovered from the genus, lending difficulty to recognizing further diversity in this morphologically cryptic genus.

Key index words: **16S rRNA gene; 16S-23S ITS; Atacama Desert; biological soil crusts; Coastal Sage Scrub; cryptic genera; cryptic species; deserts; Mojave Desert; polyphasic approach**

***Abbreviations*: BA, Bayesian Analysis; ML, maximum likelihood; MP, Maximum Parsimony; OTU, operational taxonomic units; PSRF, potential scale reduction factor; ESS, estimated sample size; CIPRES, Cyberinfrastructure for Phylogenetic Research; GTR, General Time Reversible; PAUP, Phylogenetic analysis using parsimony (and other methods); nt, nucleotide; NCBI, National Center for Biotechnology Information; NST, number of substitution types**

The uniqueness of the cyanobacterial flora of dryland soils has been highlighted in an extensive body of literature (e.g., Garcia-Pichel et al. 2001, Flechtner et al. 2008, Alwathnani and Johansen 2011, Dojani et al. 2013, Becerra-Absalón et al. 2019, Muñoz-Martín et al. 2019; also see reviews by Johansen 1993, Evans and Johansen 1999, Johansen and Shubert 2001, Büdel et al. 2016). Cyanobacteria have been the subject of significant taxonomic discovery and revision due to advances in microscopy

and DNA-based methods within the last three decades, and studies of dryland cyanobacteria have figured prominently in this effort (Flechtner et al. 2002, 2008, Řeháková et al. 2007, Perkerson et al. 2011, Mühlsteinová et al. 2014a, b, Osorio-Santos et al. 2014, Pietrasiak et al. 2014, 2019, Bohunická et al. 2015). Drylands harbor exclusive phylogenetic diversity, as some genera, such as *Mojavia*, *Kastovskya*, *Spirirestis*, *Myxacorys*, *Chroakolemma*, and *Starria* to date have only been reported for dryland soils. Yet, compared to aquatic habitats our sampling efforts are far from exhaustive, and evidence of many undescribed taxa has been commonly revealed by culture independent approaches such as clone libraries and next-generation sequencing studies (Dojani et al. 2013, Patzelt et al. 2014, Hagemann et al. 2015, Williams et al. 2016, Becerra-Absalón et al. 2019, Muñoz-Martín et al. 2019). Consequently, much more taxonomic and floristic work remains to be done, and we are still far from being able to answer broad-scale biogeographic questions with such underexplored algal biodiversity and a paucity of dryland soil cyanobacterial records.

Despite the lack of a comprehensive knowledge of fine-resolution taxonomy and biogeography, we know that the phylogenetic diversity of dryland cyanobacteria is broad. Of the eight orders currently recognized in Cyanobacteria (Komárek et al. 2014), we commonly find representation of six cyanobacterial orders in dryland soils, including: Nostocales, Oscillatoriales, Pleurocapsales, Chroococcidiopsidales, Chroococcales, and Synechococcales. Various studies have emphasized the ecofunctional importance of species in Oscillatoriales in producing copious amounts of exopolysaccharides that are necessary to stabilize the desert soil and to establish biological soil crusts (Evans and Johansen 1999, Belnap et al. 2003, Büdel et al. 2016). Further, species of Nostocales are important to dryland ecosystems as they fix atmospheric nitrogen and increase soil fertility (Dodds et al. 1995, Elbert et al. 2012, Yeager et al. 2012, Büdel et al. 2016). The functional roles of species belonging to the other orders is less clear due to our incomplete understanding of the diversity and abundance patterns of these species in soils.

Taxa in Synechococcales are commonly found in dryland soil communities and have been detected with culture dependent and independent methods (Dojani et al. 2013, Patzelt et al. 2014, Hagemann et al. 2015, Maier et al. 2018, Becerra-Absalón et al. 2019, Muñoz-Martín et al. 2019). Past researchers have hypothesized that members of this order play only minor ecological roles and contribute minimally to biomass, although some can preferentially grow in culture as "weedy" species (Rivera-Aguilar et al. 2006, Becerra-Absalón et al. 2019, Giraldo-Silva et al. 2019). Although ecological roles may still be unknown, indications of thermal and desiccation tolerance of simple filamentous members in Synechococcales, especially in the genera *Leptolyngbya*, *Trichocoleus*, and *Schizothrix,* have been discovered and discussed (Hagemann et al. 2015, Muñoz-Martín et al. 2019).

Leptolyngbya is an especially interesting case for biogeography and α–level taxonomy studies, as it is a species rich heterogeneous genus reported as ubiquitous in all aquatic and terrestrial habitats exposed to light (Komárek and Anagnostidis 2005). *Leptolyngbya* species are unbranched, nonheterocytous, filamentous cyanobacteria that are character poor. A simple morphology, phenotypic plasticity of traits such as sheath development and false branching, and a broad morphological circumscription of the genus have been the cause of much taxonomic confusion causing classification challenges with *Leptolyngbya*-like taxa. Over the past three decades taxonomic studies of many strains and species initially identified as *Leptolyngbya* species led to the discovery and repeated confirmation of the polyphyly in this genus (Turner 1997, Casamatta et al. 2005, Taton et al. 2006, Johansen et al. 2008, 2011, Vaz et al. 2015). Applying the polyphasic approach, including DNA-based characterizations, led to revisions of the genus with many dryland taxa belonging to diverse genus level clades outside *Leptolyngbya* sensu stricto. Recent examples of newly discovered and described dryland taxa include: *Chroakolemma* spp., *Drouetiella fasciculata*, *Kaiparowitsia implicata*, *Nodosilinia* spp., *Oculatella* spp., *Pegethrix* spp., *Timaviella* spp., and *Trichocoleus desertorum*, (Perkerson et al. 2011, Mühlsteinová et al. 2014a,b, Osorio-Santos et al. 2014, Becerra-Absalón et al. 2018, Mai et al. 2018).

Over the past 10 years we have isolated and maintained several cyanobacterial strains morphologically corresponding to *Leptolyngbya foveolarum* from American drylands. Colonies of this taxon were bright turquois blue-green with a glistening appearance, and curving, entangled filaments spreading flat on the agar away from the colony center. The sheath enclosing individual trichomes was colorless and firm. Cells were typically isodiametric to shorter than wide. After DNA extraction, cloning, and sequencing of the 16S rRNA gene region, all strains previously identified as *L. foveolarum* fell in a well-supported monophyletic clade outside of *Leptolyngbya* sensu stricto but within Synechococcales. Herein we describe and characterize this clade as *Trichotorquatus* gen. nov., including the description of four new species from dryland soils in North and South America.

MATERIALS AND METHODS

Sample collection. Soil samples yielding all cyanobacterial isolates investigated in this paper were collected throughout the past ten years from North and South American semi-arid and arid drylands including locations in Joshua Tree National Park in Summer 2006 ("WJT" strains), Atacama Desert in Austral Autumn 2009 ("ATA" strains), Mojave National Preserve in Spring of 2010 and 2011 ("CMT" strains), and Santa

Margarita Ecological Reserve near San Diego in Summer 2013 ("SMER" strain; Table S1 in the Supporting Information). All soils were collected air-dry and stored at room temperature in the laboratory until enrichment culturing.

Strain isolation and morphological characterization. Each soil collection was well mixed and subsampled to obtain a representative 1 g soil sample for dilution plating. Each WJT, CMT, and ATA subsample was suspended in 100 mL of liquid Z-8 medium (Carmichael 1986), shaken on a shaker table for 4 h, and dilution plated onto agar-solidified Z-8 medium. After 6-12 weeks of incubation at 16:8 h light:dark cycle at 16°C under fluorescent light, colonies were picked from enrichment plates and isolated into tubes containing either liquid or agar-solidified Z-8 media to obtain unialgal cultures. Samples of biological soil crust from SMER were ground in a mortar and pestle, serially diluted in BG-11 medium in 24-well plates and incubated at 30°C under fluorescent light. Inoculum from the limiting dilution was isolated by repeated streaking onto solid BG-11 medium (1.5% agar), and cultures were maintained in liquid BG-11 medium. Cultures have been maintained since isolation at 16:8-hr light:dark cycle in a growth room at 16°C at John Carroll University (JCU). Sub-cultures of these cultures were sent to New Mexico State University (NMSU) in 2015 and these sub-cultures have been maintained at room temperature in a lighting shelf there.

All comparative morphological observations were performed on NMSU cultures. Observations on colony morphology were made with a MEIJI EMZ-5TR dissecting microscope and photographed using AmScope MU1603 camera. Colony observations were made using cultures grown in liquid and solid media during exponential growth phase. Cell morphology was studied and photographed with a Zeiss AxioImager.A2 microscope equipped with Nomarski differential interference contrast optics and a Zeiss Axiocam 305 color camera. Using a common garden design we compared cell morphology of all species at 1, 3, and 4 weeks, and in mature stationary phase at 4-6 months after transfer for both agar and liquid Z-8 medium.

Type material preparation. Type materials were prepared by filtering living cultures through a 23 mm glass-fiber filter, allowing the filter to air-dry for a week, and then placing the filter in a herbarium envelope for deposit in the NMSU Herbarium (NMC – see Thiers 2020). Each holotype was accompanied by isotype material preserved in a 4% formaldehyde solution. Paratypes collected from different sites were prepared in the same manner as holotypes. Reference strains for all for species have been deposited in the UTEX Algal Culture Collection. At the time this manuscript went to press they were in process of incorporation into the collection and consequently accession numbers were not yet available. The authors placed no restrictions of their own on their distribution for research.

DNA-based characterization. We extracted DNA from all strains investigated using the UltraClean Microbial DNA Isolation Kit (MO BIO Laboratories, Carlsbad, CA, USA; analog to the modern day DNeasy UltraClean Microbial Kit, Qiagen, Hilden, Germany) employing vortex cell disruption and following the manufacturer's protocols. If DNA extraction was unsuccessful with the UltraClean Kit we extracted DNA with a modified cetyl trimethylammonium bromide (CTAB) protocol using bead beating following Burke et al. (2006). DNA was then amplified targeting the 16S rRNA and 16S-23S ITS gene region of the ribosomal operon with a length of about 1600 nucleotides using the forward primer CYA359F 5'-GGGGAATTTTCCGCAATGGG-3' and reverse primer 1 5'-CTCTGTGTGCCTAGGTATCC-3' (Wilmotte et al. 1993, Nübel et al. 1997, Boyer et al. 2001, 2002). PCR reactions were prepared with 1X GoTaq® Flexi Buffer, 0.025 units · μL^{-1} GoTaq® Flexi DNA Polymerase, 3 mM MgCl2 (Promega, Madison, WI, USA), 0.2 mM dNTPs, 0.5 $\mu g \cdot \mu L^{-1}$ of BSA (NEB, Ipswich, MA, USA) and 0.5 µM each of the forward and reverse primer (Eurofins). PCR was run in a Bio-Rad PCR Thermocycler (Bio-Rad laboratories, Inc., France) with a 3-min incubation at 94°C to minimize non-specific DNA amplifications. Subsequently, reactions underwent 35 cycles of 94°C (30 s), 53°C (30 s) and 72°C (60 s), followed by an incubation at 72°C (300 s) to complete synthesis. Following PCR, products were cloned with the StrataClone PCR cloning kit (La Jolla, CA, USA) according to manufacturer recommendations. At least four *E. coli* colonies per strain were picked. Plasmid DNA was extracted and purified with QIAPrep Miniprep Spin kit (Qiagen, Carlsbad, CA, USA). EcoRI digestion was performed to select successful clones. If possible, we selected at least two clones of each strain. More clones were chosen if a different digestion patterns was detected indicating potential operon variability. Selected clones were sequenced using Sanger sequencing technology with five internal sequence primers including M13 forward, M13 reverse, primer 5 (5'-TGT ACA CAC CGG CCC GTC-3'; Wilmotte et al. 1993), primer 7 (5'-AAT GGG ATT AGA TAC CCC AGT AGT C-3') and primer 8 (5'-AAG GAG GTG ATC CAG CCA CA-3'; Nübel et al. 1997) by Functional Biosciences, Inc. (Madison, WI, USA). For each submitted clone, associated raw sequence reads were aligned, error proofed, and assembled to contigs using the Sequencher Software (version 4.8; Ann Arbor, MI, USA). Assembled clone sequences were submitted to NCBI's GenBank database (see GenBank numbers in Table S2 in the Supporting Information).

Phylogenetics and secondary structure modeling. An alignment with 329 16S rRNA sequences representing Oculatellaceae (96 sequences), Leptolyngbyaceae (109 sequences), Prochlorotrichaceae (90 sequences), and Trichocoleusaceae (9 sequences) was assembled using ClustalW (Larkin et al. 2007), with manual correction where necessary to maintain secondary structure of the 16S rRNA helices. *Gloeobacter violaceus* and *Thermostichus bigranulatus* were used as outgroup taxa. Phylogenetic analyses were conducted using the CIPRES Science Gateway (Miller et al. 2015). Maximum likelihood (ML) analysis was conducted using RAxML, employing the GTR+I+Γ model, with 1000 bootstrap replications. Bayesian Inference (BI) analysis was conducted using MrBayes on XSEDE (3.2.7a) employing the TPM2uf model identified by jModeltest (Darriba et al. 2012) as the best model for this dataset, with 50 million generations, as well as with the GTR+I+Γ model, with 50 million generations. The phylogeny reported is the BI analysis with the TPM2uf model, with bootstrap values from the ML analysis mapped on to the tree. The BI analysis achieved an average standard deviation of split frequencies of 0.0247. The potential scale reduction factor (PSRF) was 1.00 for all parameters, indicating chains converged, and the minimum estimated sample size (ESS) was >300 for all parameters, indicating all parameters were adequately sampled in this analysis.

Next, 16S-23S ITS gene regions were inspected for operon variability and three orthologous sets of 16S-23S ITS regions were identified, indicating that *Trichotorquatus* species likely have at least three ribosomal operons, one with both tRNA genes present in the region, and two lacking tRNA genes. Alignments for each orthologous set were constructed using a combination of ClustalW and manual alignment, such that the conserved domains all remained aligned. Maximum Parsimony (MP) was conducted using PAUP ver. 4b10 (Swofford 1998). For this analysis, indels were counted as a fifth base following standard phylogenetic methods for cyanobacterial ITS sequence data (Perkerson et al. 2011, Osorio-Santos et al. 2014, Bohunická et al. 2015, Mareš et al. 2019,

Becerra-Absalón et al. 2020, Mesfin et al. 2020, Shalygin et al. 2020). A total of 10,000 bootstrap replicates were obtained for this analysis. This was done for all three operons. In the second set of analyses, sequences of the 16S-23S ITS region of the operon containing both tRNA genes were aligned with indels coded (0 for gap, 1 for nucleotide), and an unrooted phylogenetic tree was obtained with a BI analysis with 52,000 generations discarding the first 25% of samples as burn-in, choosing NST = MIXED, and applying the GTR+I+Γ evolutionary model. Average standard deviation of split frequencies was 0.00482 and the PSRF for this analysis was ≤1.014 for all parameters. A BI analysis using the same parameters was completed for an alignment of the 16S-23S ITS region of operon 2 containing no tRNA genes (19 distinct sequences of *Trichotorquatus*). With 410,000 generations, the average standard deviation of split frequencies was 0.00494 and the average PSRF for this analysis was ≤1.001 for all parameters. Finally, a BI analysis using the same parameters was completed for an alignment of the 16S-23S ITS region of operon 3 containing no tRNA genes (7 distinct sequences of *Trichotorquatus*). With 102,000 generations, the average standard deviation of split frequencies was 0.00492 and the average PSRF was ≤1.020 for all parameters. For all ITS phylogenies, the BI topology is shown, with MP bootstrap values mapped on to the tree. All phylogenies were visualized in FigTree (Rambaut 2018), and subsequently edited in Adobe Illustrator (San Jose, CA). Secondary structures of the D1-D1', Box-B, and V3 helices were predicted with Mfold (Zuker 2003). All Mfold structures were compiled for each helix and redrawn in Adobe Illustrator.

RESULTS

Trichotorquatus *Pietrasiak & J.R.Johansen gen. nov.. Diagnosis*: Differing from the sister genus *Kaipairowitsia* ecologically in its occurrence only in desert soils and morphologically by having wider cell dimensions and differing cell shape, cells of *Trichotorquatus* being in general isodiametric to shorter than wide while cells of *Kaipairowitsia* are in general longer than wide (Figs. 1-6). *Trichotorquatus* also lacks the *Arthronema*-like outgrowths and presence of multiple trichomes in a single sheath typical for *Kaipairowitsia*. Morphologically, closest to *Leptolyngbya* sensu stricto, but phylogenetically distant from that taxon.

Description: Colony forming a floating mat in liquid culture by capturing oxygen bubbles during photosynthesis, on agar not penetrating the substrate, but occasionally with upright solitary filaments. Filaments always with a single trichome, only rarely producing pseudobranches, flexuous or straight, not typically entangled. Sheath colorless, firm, thin to variable in thickness, adhering tightly to the trichome, sometimes absent at the ends, often forming a distinctive telescoping collar near trichome apices or a telescoping frayed appearance along the mid-region of the filament, often distinctively kinked and bent, persistent after trichome escapes from sheath. Trichomes slightly constricted to constricted at the crosswalls, with constrictions visible only when sheath is absent, up to 4.3 μm wide. Cells isodiameteric to longer than wide, rarely shorter than wide (only immediately after cell division), with thylakoids either parietal or in strand-like fascicles extending longitudinally through the centroplasm, typically with nongranular cell contents, sometimes with one or two minute granules visible at the crosswalls, bright turquoise blue-green cell contents in healthy cultures, becoming yellowish in senescent cultures. Apical cells rounded, longer on average than vegetative cells, sometimes with paler coloration, otherwise not morphologically distinct from vegetative cells. Necridia present, often in rows.

Etymology: *Trichotorquatus* L. = Collared trichome, named for the telescoping sheath at the apex of many trichomes forming a collar around the trichome.

Type species: *Trichotorquatus maritimus* sp. nov.

Taxonomic note: The designation *Trichotorquatus* was used as a provisional name in a conference paper and was subsequently listed in Komárek et al. 2014 as a provisional name. It was not accompanied by a description or diagnosis, nor was a type designated. It was referred to as a "provisional" name and is thus invalid (ICN Art. 32; Turland et al. 2018). This designation is validly published herein.

Trichotorquatus maritimus *Pietrasiak, S.Reeve & J.R.Johansen sp. nov.. Description: Morphology in culture*: Colony dark turquoise green, flatly spreading on agar medium with few upright solitary filaments (Figs. 1, A–L; 3, A–K; 5, D, E, L and M; 6, D and E). Filaments mostly unbranched, single and double false branching rarely observed, with a single trichome in each sheath, 2.2-7.3 μm wide (mean=3.1 μm wide). Sheath typically thin, sometimes widened, firm and rigid, sometimes absent, 0.2-2.4 μm thick when present, often having a telescoping frayed appearance along the length of the trichome. Trichomes bright turquoise green, distinctly constricted at the crosswalls, fragmenting at necridia or at simple separating cell divisions, 2.1-4.3 μm wide (mean= 2.8 μm wide). Cells with distinct chromoplasm and centroplasm, with thylakoids either parietal or in strand-like fascicles extending longitudinally through the centroplasm, 0.9-10.0 μm long (mean=2.5μm long), dividing cells up to 9.4 μm long, with some non-dividing cells abnormally elongated up to 26 μm long. Apical cell blue-green, 2.2-32 μm long (mean=4.7 μm long). Necridia often in rows, forming sections up to 32 μm long. Hormogonia very short, often with 1-6 cells, produced under all culture conditions.

ITS secondary structure: D1-D1' helix 80 nucleotides long in operon 2 (no tRNA genes), with a basal clamp of five base pairs (5'-GACCU–AGGUC-3'). D1-D1' helix 64 nucleotides long in operon 3 (no tRNA genes), with a larger subterminal bilateral bulge than all other species for which operon 3 was recovered. Box-B helix in operon 2 distinctly differing in structure and sequence from *Trichotorquatus coquimbo* and *T. ladouxae*, but identical in structure

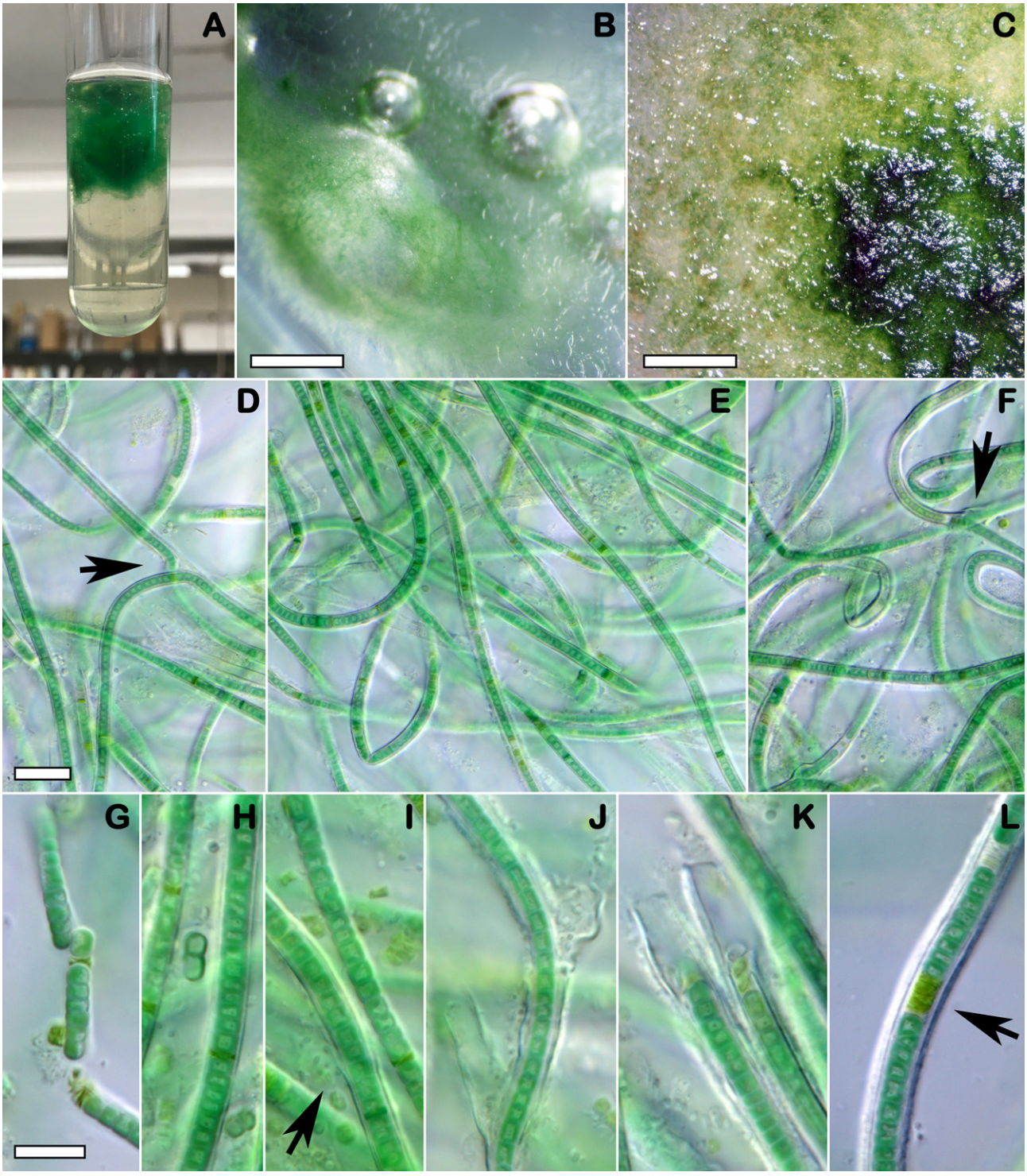

FIG. 1. *Trichotorquatus maritimus*. (A, B) Colony morphology showing floating colony in liquid culture due to entrapment of oxygen in the mucilage of the mat. (C) Mat morphology on agar. (D) Filament with double false branching (arrow), (E, F) Filaments at low magnification, showing collared sheath (arrow). (G, H) Filaments at higher magnification, showing hormogonia (G, H), collared sheath (I, arrow), fraying sheath (J), expanded end sheath (K) and rows of necridia (L, arrow). Scale bars B, C: 1 mm; D–F: 20 μm, G–L: 10 μm. [Colour figure can be viewed at wileyonlinelibrary.com]

to *T. andrei,* from that taxon differing only in one nucleotide in the terminal loop. Box-B helix in operon 3 distinctly longer than Box-B helices in other taxa, with a unilateral bulge on the 3' side of the helix. V3 helix distinct in many regards from V3 helices in other taxa in all orthologous operons.

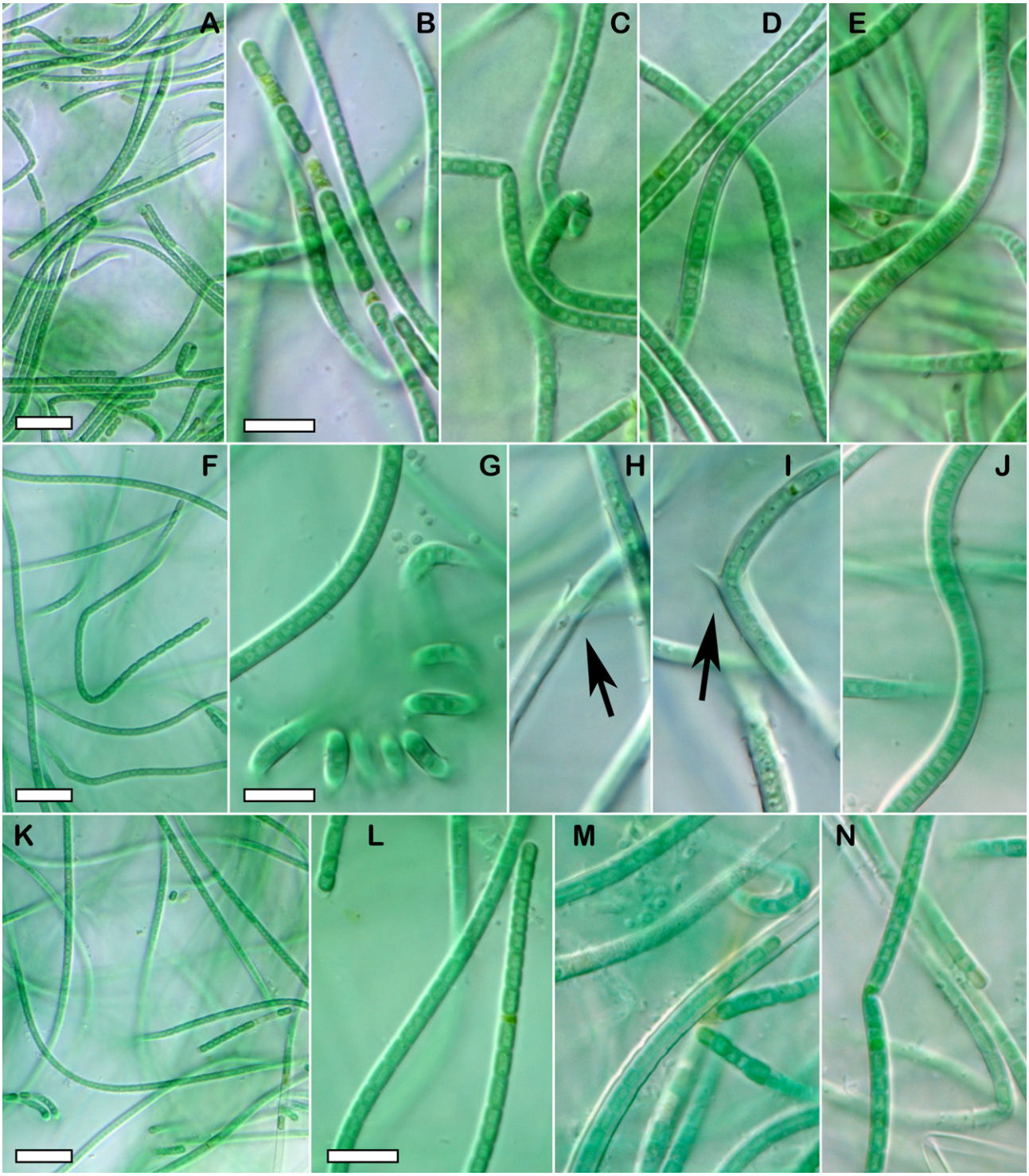

FIG. 2. *Trichotorquatus* species. (A–E) *T. coquimbo*. (F–J) *T. andrei*, showing collared sheath (H, I, arrows). (K–N) *T. ladouxae*. Scale bars A, F, K: 20 μm, B–E; G–J, L, M: 10 μm. [Colour figure can be viewed at wileyonlinelibrary.com]

Etymology: *Maritimus*, named for the maritime climate of San Diego, California, the site of origin for this species.

Holotype here designated: NMC 109455, dried biomass of the reference strain, SMER-A, prepared on a glass-fiber filter. Isotype material included in accession NMC 109455 is material preserved in 4% formaldehyde.

Type locality: Santa Margarita Ecological Reserve (SMER), located in northern San Diego County and

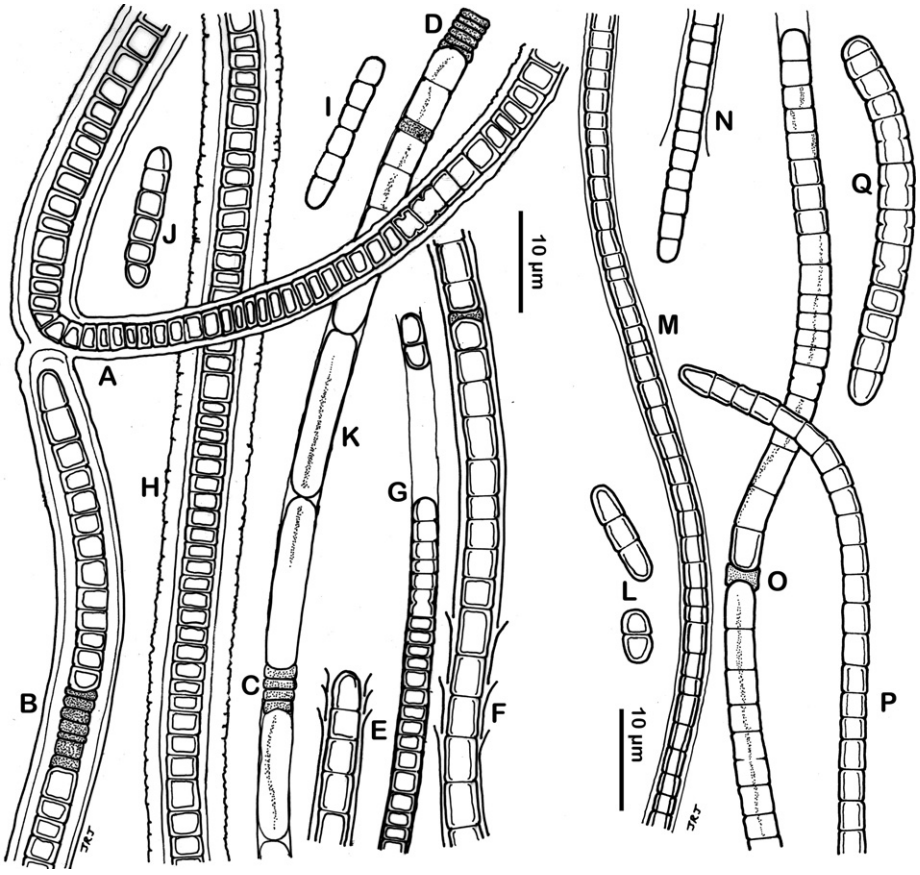

FIG. 3. *Trichotorquatus maritimus* (A–K) and *T. coquimbo* (L–Q). A. Single false branching. (B–D) Rows of necridia. (E, F) Telescoping collar-like sheaths. (G) Filament with thin sheath. (H) Filament with thick, rigid sheath. (I, J) Hormogonia. (F) Cells with longitudinally arranged fascicles of thylakoids. (L) Hormogonia. (M) Filament with trichome with parietal thylakoids. (N) collared sheath. (O) necridium. (P) Sheathless trichome. (Q) Actively dividing cells. All images to same scale.

southern Riverside county near the cities of Temecula and Fallbrook, 33°26'28" N, 117° 9'52" W, elevation 388 m. Biological soil crusts in coastal sage scrub. Sampled June 20, 2013, by Sharon Reeve.

Reference strain: SMER-A. Culture isolated by Sharon Reeve.

GenBank accession number: MK188321.

Trichotorquatus coquimbo *Osorio-Santos, Pietrasiak & J.R.Johansen sp. nov.. Description: Morphology in culture*: Colony dark turquoise, with occasionally raised solitary filaments (Figs. 2, A–E; 3, L–Q; 5, A and I; 6A). Filaments unbranched, with a single trichome in each sheath, 2.2-3.6 µm wide (mean = 2.6 µm wide). Sheath sometimes absent, 0.1-0.6 µm thick when present, rarely with short telescoping collar near trichome apices, smooth along the length of the filament. Trichomes bright turquoise green, distinctly constricted at the crosswalls, fragmenting at necridia or at simple separating cell divisions, 1.8-3.4 µm wide (mean= 2.5 µm wide). Cells with distinct chromoplasm and centroplasm, with thylakoids either parietal or in strand-like fascicles extending longitudinally through the centroplasm, 1.2-5.6 µm long (mean=2.4 µm long), dividing cells up to 4.6 µm long. Apical cell pale yellowish green, 1.6-5.0 (mean=3.0 µm long). Necridia often in rows, forming sections up to 4.9 µm long. Hormogonia short, often with 4-10 cells.

ITS secondary structure: D1-D1' helix 101 nucleotides long, longer than D1-D1' helix in any other species, with a basal clamp of six base pairs (5'-GACCUU–AAGGUC-3'). Box-B helix differing slightly in structure from other Box-B helices in operons 1 and 2 of all other species due to a single A to U transversion mutation at nucleotide 32, as well as a single transition mutation in the terminal loop at nucleotide 18. V3 helix with a basal clamp of 3 base pairs (5'-GUC–GAC-3') followed by a small mismatch (5'-AG–A-3') as in all other V3 helices, but differing from V3 helices in operons 1 and 2 of all other species due to the abundance of bilateral bulges, with three large (9-12 unpaired nucleotides) and two smaller (5-6 unpaired nucleotides) internal openings. Operon 3 not recovered for this species.

Etymology: *Coquimbo*, named for the Coquimbo Region of the Atacama Desert.

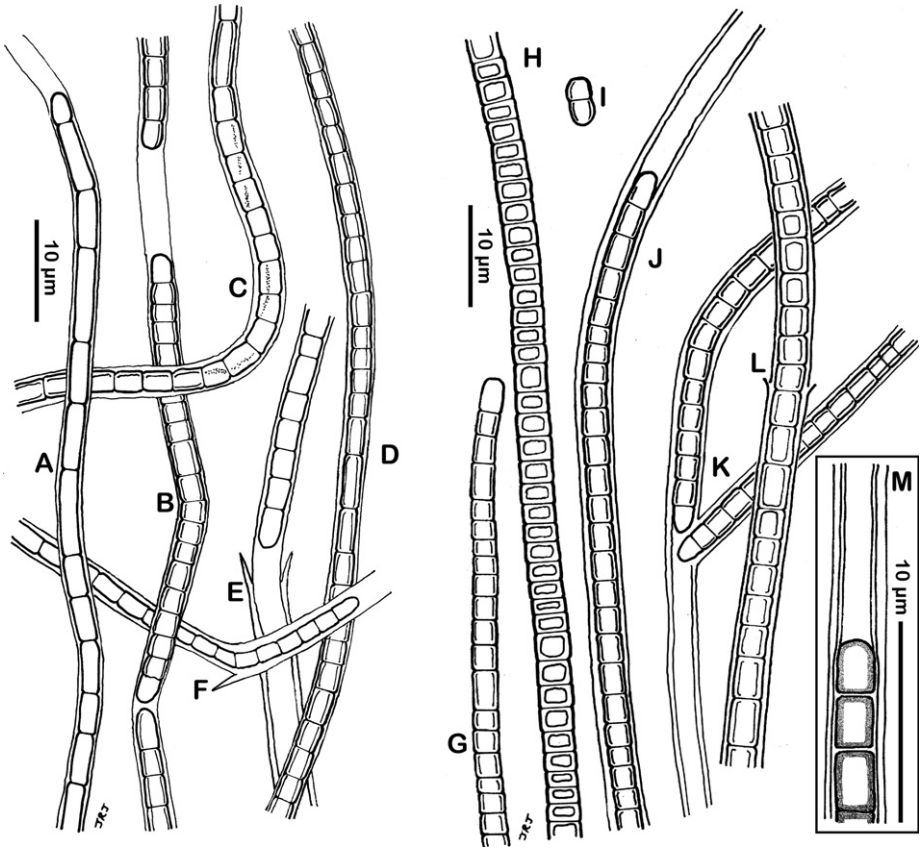

FIG. 4. *Trichotorquatus andrei* (A–F) and *T. ladouxae* (G–M). (A) Elongated cells. (B) Filaments with thin sheath and parietal thylakoids. (C, D) Cells with longitudinally arranged fascicles of thylakoids. (E, F) Collared sheaths. (G) Trichome lacking sheath with parietal thylakoids along outside walls. (H) Trichome lacking sheath with parietal thylakoids along outside walls and cross walls. (I) Hormogonium. (J) Filament with typical sheath. (K) Single false branching. (L) Collared sheath. (M) Higher magnification view showing stratified sheath (inset).

Holotype here designated: NMC109461, dried biomass of the unialgal reference strain, ATA2-1-KO25A, prepared on a glass-fiber filter. Isotype material included in accession NMC 109461 is material preserved in 4% formaldehyde.

Type locality: Biological soil crust near Choros Bajos, 29°18'59.34" S, 71°14'55.14" W, elevation 215 m. Sampled 12 May 2009, by Karina Osorio-Santos, Jeffrey R. Johansen, Lauren Baldarelli, Karen Godoy, and Steve Warren.

Reference strain: ATA2-1-KO25A. Culture isolated by Karina Osorio-Santos.

Other strains: ATA2-1-CV25A.

GenBank accession number: MK188309.

Trichotorquatus andrei *Pietrasiak et J.R.Johansen sp. nov.*. *Description: Morphology in culture*: Colony dark turquoise, with occasionally raised solitary filaments (Figs. 2, F–J; 4, A–F; 5, B, F, J and N; 6, B and F). Filaments unbranched, with a single trichome in each sheath, 1.6-5.6 µm wide (mean=2.7 µm wide). Sheath sometimes absent, 0.2-3.0 µm thick when present, smooth, frequently wide enough to see trichomes clearly. Trichomes bright turquoise green, distinctly constricted at the crosswalls, fragmenting at necridia or at simple separating cell divisions, 1.0-2.8 µm wide (mean= 2.1 µm wide). Cells with distinct chromoplasm and centroplasm, with thylakoids either parietal or in strand-like fascicles extending longitudinally through the centroplasm, 1.5-5.0 µm long (mean=2.9 µm long), dividing cells up to 5.4 µm long, with some non-dividing cells elongated up to 12.4 µm long. Apical cell often more yellowish than vegetative cells, 1.4-6.3 µm long (mean=3.2 µm long). Necridia often in rows, forming sections up to 11 µm long. Hormogonia typically 4-8 cells long.

ITS secondary structure: D1-D1' helix 80 nucleotides long in both operons 1 and 2, with a basal clamp of five base pairs (5'-GACCU–AGGUC-3'), closest in structure to the D1-D1' helix in *Trichotorquatus ladouxae*, but differing in the larger bilateral bulge mid-helix. D1-D1' helix in operon 3 identical to that in *T. ladouxae*, differing in a single base pair in mid-helix. Box-B helix differing slightly in structure from other Box-B helices in operons 1 and 2 of *T. coquimbo* and *T. ladouxae*, but very similar in sequence to *T. maritimus*. V3 helix in operons 1 and 2 very similar to the V3 helix in *T. ladouxae*, but differing slightly in structure and sequence in

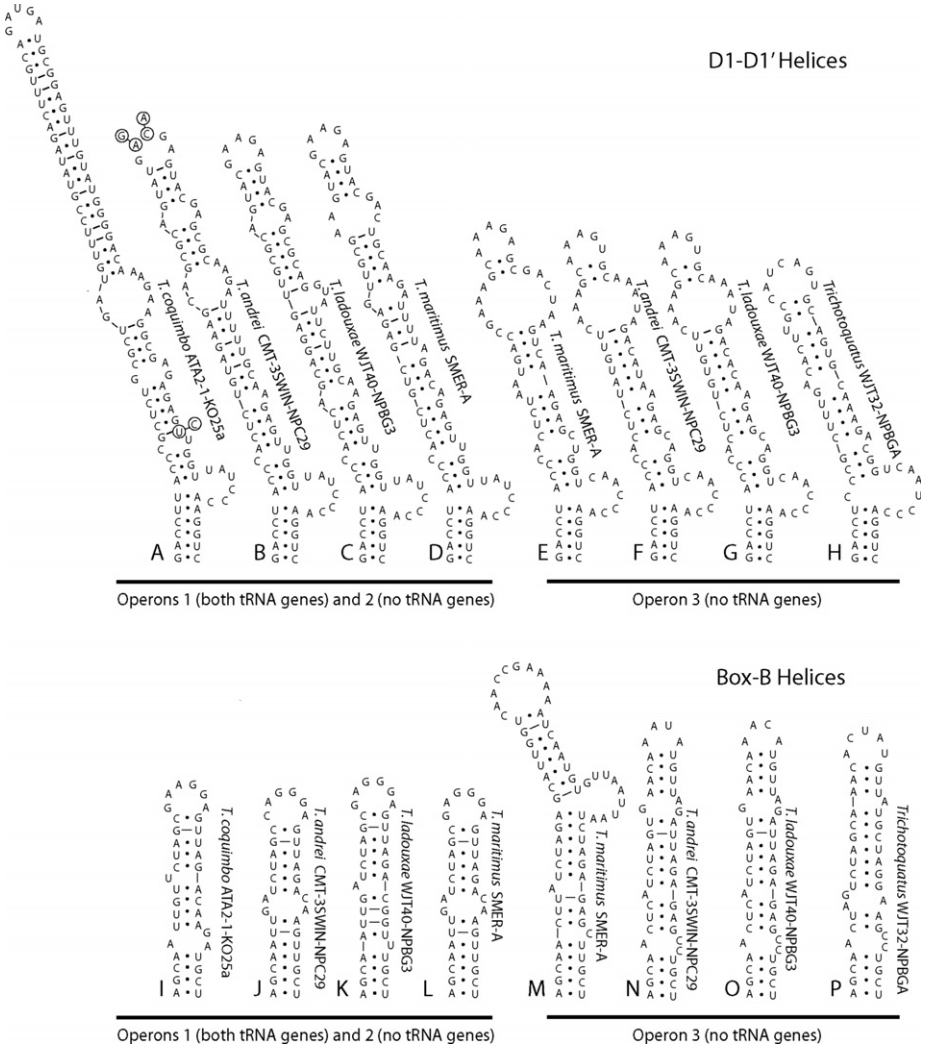

FIG. 5. Secondary structures for conserved helices in the 16S-23S ITS regions of *Trichotorquatus* species. (A–H) D1-D1' helices for Type 1 (both tRNA genes), Type 2 (no tRNA genes), and Type 3 (no tRNA genes) operons. I-P) Box-B helices for Type 1 (both tRNA genes), Type 2 (no tRNA genes), and Type 3 (no tRNA genes) operons. Labels for species and strains are shown to the right of each structure. The sequence for Type 1 structure is shown as the basal structure when both Type 1 and Type 2 operons were recovered (*T. coquimbo, T. andrei, T. ladouxae*), with the nucleotide substitutions in the Type 2 operon shown in circles where different from the corresponding Type 1 sequence. *T. andrei* strain CMT-3SWIN-NPC29 and *T. ladouxae* strain WJT40-NPBG3 had all three operons types available and were chosen to represent these two species. The type strains had identical Type 2 structures to those selected strains. Only Type 2 and Type 3 operons were recovered for *T. maritimus*, and only the Type 3 operon was recovered for *Trichotorquatus* sp. 5. Additional strains within these species had identical structures within species, but sometimes differed by 1-2 nucleotides.

mid-helix. V3 helix in operon 3 most similar to that in *T. ladouxae*, but possessing one fewer small bilateral mismatches.

Etymology: *Andrei*, named in honor of Jim Andre, Director of the Granite Mountains Research Station and good friend of the authors.

Holotype here designated: NMC 109459, dried biomass of the reference strain, WJT9-NPBG15, prepared on a glass-fiber filter. Isotype material included in accession NMC 109459 is material preserved in 4% formaldehyde.

Paratype here designated: NMC 109460, dried biomass of the reference strain, CMT-3SWIN-NPC38, prepared on a glass-fiber filter. Paratype material included in accession NMC 109460 is material preserved in 4% formaldehyde.

Type locality: Site WJT9, Fried Liver alluvial fan in Joshua Tree Nat. Park, CA. Mojave Desert, USA, 33°52'34" N, 115°54'35" W, elevation 700 m. Sandy, gravelly soil from mixed parent material, algal and lichen crust present but not common, plants present.

Collected June 1, 2006 by Nicole Pietrasiak.

Reference strain: WJT9-NPBG15. Culture isolated by Nicole Pietrasiak.

Other strains: CMT-3FSIN-NPC33, CMT-3FSIN-NPC37, CMT-3SWIN-NPC29, WJT19-NPBG5, WJT54-NPBG7, WJT55-NPBG7.

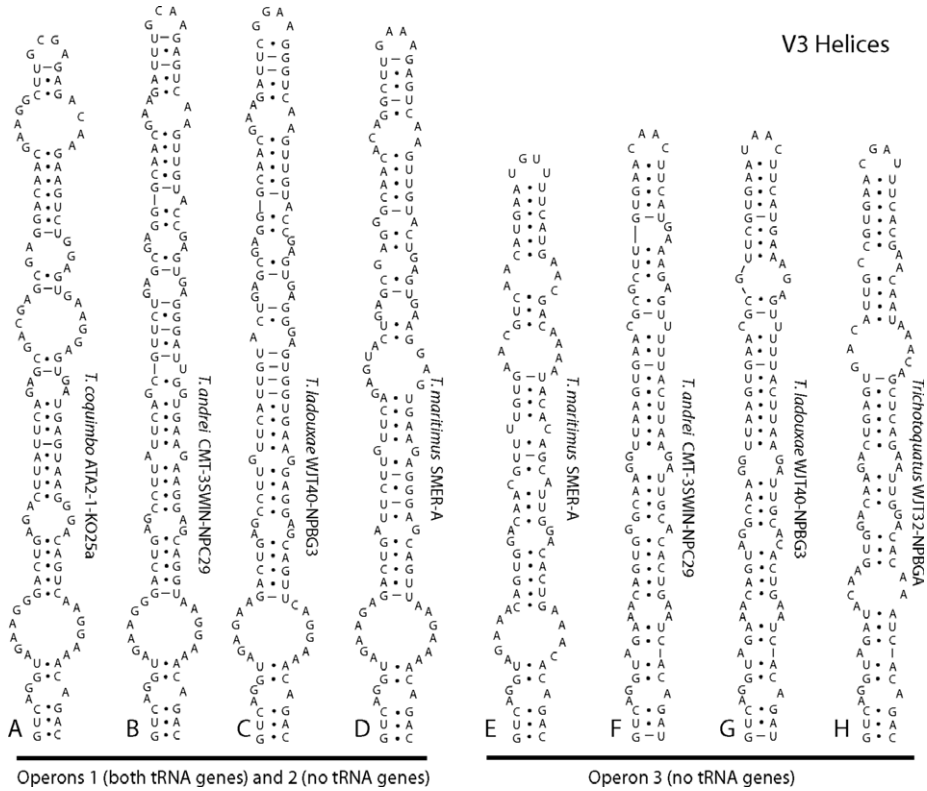

FIG. 6. Secondary structures for V3 helices in the 16S-23S ITS regions of *Trichotorquatus* species. (A–D) V3 helices for Type 1 (both tRNA genes) and Type 2 (no tRNA genes) operons. E-H) V3 helices for Type 3 (no tRNA genes) operons. Differences within species between Type 1 and 2 operons not detected. Additional strains within these species had identical structures within species, but sometimes differed by 1-2 nucleotides.

GenBank accession number: MK188324.

Trichotorquatus ladouxae *Pietrasiak et J.R.Johansen sp. nov. Description: Morphology in culture*: Colony dark turquoise, with occasionally raised solitary filaments (Figs. 2, K–N; 4, G–M; 5, C, G, K and O; 6, C and G). Filaments mostly unbranched, pseudobranches present but rare, with a single trichome in each sheath, 2.0-7.0 μm wide (mean=3.1 μm wide). Sheath sometimes absent, 0.2-3.0 μm thick when present, smooth to rough appearance along the length of the trichome. Trichomes bright turquoise green, distinctly constricted at the crosswalls, fragmenting at necridia or at simple separating cell divisions, 2.0-3.6 μm wide (mean= 2.6 μm wide). Cells with distinct chromoplasm and centroplasm, with thylakoids either parietal or in strand-like fascicles extending longitudinally through the centroplasm, 1.2-4.0 μm long (mean=2.4 μm long), dividing cells up to 4.4 μm long. Apical cell blue-green, 1.8-4.6 μm long (mean=3.1 μm long). Necridia often in rows, forming sections up to 12 μm long. Hormogonia short, typically under 10 cells long.

ITS secondary structure: D1-D1' helix 80 nucleotides long in both operons 1 and 2, with a basal clamp of five base pairs (5'-GACCU–AGGUC-3'), closest in structure to the D1-D1' helix in *Trichotorquatus andrei*, but differing in the possession of a small unilateral bulge on the 3' strand in mid-helix. D1-D1' helix in operon 3 identical to that in *T. andrei*, differing in a single base pair in mid-helix. Box-B helix differing in structure from other Box-B helices in operons 1 and 2, but identical to that of *T. andrei* in operon 3. V3 helix in operons 1 and 2 similar to the V3 in *T. andrei*, but differing slightly in structure and sequence in mid-helix. V3 helix in operon 3 also most similar to that in *T. andrei,* but differing in sequence and structure in the terminal 24 nucleotides.

Etymology: *Ladouxae*, named in honor of Tasha LaDoux, who facilitated our research in Wonderland of Rocks, Joshua Tree National Park and ever since has been a dear friend of the authors.

Holotype here designated: NMC 109456, dried biomass of the reference strain, WJT36-NPBG11, prepared on a glass-fiber filter. Isotype material included in accession NMC 109456 is material preserved in 4% formaldehyde.

Paratype here designated: NMC 109457, dried biomass of the reference strain, WJT40-NPBG3, prepared on a glass-fiber filter. Paratype material included in accession NMC 109457 is material preserved in 4% formaldehyde.

Type locality: Site WJT36, Wonderland of Rocks. in Joshua Tree Nat. Park, CA. Mojave Desert, USA,

34°02'29'' N, 116°08'42'' W, elevation 1327 m. Sandy, gravelly soil from granitic outcrops, plants and well-developed algal crusts. Sampled June 28, 2006 by Nicole Pietrasiak.

Reference strain: WJT36-NPBG11. Culture isolated by Nicole Pietrasiak.

Other strains: WJT66-NPBG9, TAA2-2HA1-27.2.

GenBank accession number: MK188326.

Trichotorquatus *species 5 (WJT32-NPBGA). Comment: Morphology in culture*: Filaments unbranched, pseudobranches unobserved, with a single trichome in each sheath, 2.0-4.0 μm wide (Figs. 5, H and P; 6H). Sheath sometimes absent, 0.2-0.6 μm thick when present, smooth appearance along the length of the trichome. Trichomes bright turquoise green, indistinctly to distinctly constricted at the crosswalls, 2.0-2.8 μm wide. Cells with distinct chromoplasm and centroplasm, with parietal thylakoids, mostly isodiametric to shorter than long, 1.6-6.0 μm long. Apical cell blue-green. Hormogonia short, under 10 cells long.

ITS secondary structure: D1-D1' helix 57 nucleotides long in operon 3, with a basal clamp of five base pairs (5'-GACCU–AGGUC-3'), differing in structure to the D1-D1' helix of that operon in all other strains through the absence of the large subterminal bilateral bulge and the absence of the small bilateral bulge above the basal clamp and 3' unilateral bulge, as well as in having 8 nucleotides in the 3' unilateral bulge (as opposed to 7 in all others) opposite a single cytosine residue. Box-B helix differing in structure from all other Box-B helices in operon 3, but with nucleotide number (44) close to that in *Trichotorquatus coquimbo, T. andrei*, and *T. ladouxae* (45 in all three). V3 helix in operons 3 with one nucleotide less than in all other species and differing in secondary structure from all other species based upon the bilateral bulges present in the helix. Operons 1 and 2 not recovered.

Due to contamination with another cyanobacterium, this strain was lost early and type material is not available. Furthermore, complete morphological characterization was not possible and only a single ribosomal operon was recovered. This strain is considered incompletely characterized with regards to both morphology and molecular sequence data. However, based on the significant differences in secondary structure and length of the conserved domains of the 16S-23S ITS, as well as phylogenetic position, this strain represents a new but as yet undescribed species in *Trichotorquatus*.

Phylogenetic and ITS analysis: Bayesian Inference and Maximum Likelihood analysis of the 16S rRNA gene using 329 sequences generally agreed with each other and tree topology revealed *Trichotorquatus* as a well-supported clade (Bayesian posterior probabilities = 1.00, Maximum Likelihood bootstrap values = 100, Fig. 7, Fig. S1 in the Supporting Information) in the Oculatellaceae family similar to the phylogenetic results in Mai et al. (2018). Specifically, *Trichotorquatus* is sister to *Kaiparowitsia* with a ≤92.2% 16S rRNA gene sequence similarity to its sister clade (Table S3 in the Supporting Information). The clade containing *Trichotorquatus* and *Kaiparowitsia* was also highly supported with Bayesian posterior probabilities = 0.97. Both genera were sister to the other genera in Oculatellaceae including *Pegethrix, Cartusia, Elainella, Drouetiella, Timaviella, Oculatella, Tildeniella, Komarkovaea,* and *Thermoleptolyngbya* (Fig. 7). The Oculatellaceae clade was well supported (1.00/79). This phylogeny did not distinguish *T. andrei* from *T. ladouxae*, which formed a clade well separated from *T. maritimus*, *T. coquimbo* and *Trichotorquatus* sp. 5.

Three distinct operons were recovered based on sequence differences in the 16S-23S ITS region. The first two operons were easily separated as the Type 1 operon had two tRNA genes, whereas the Type 2 operon had none. Both of these operons shared the typical start sequence of the 23S rRNA gene (5'–GGTCAAGWTAATAAG–3'). The Type 3 operon also had no tRNA genes and was recognizable by the fact that the beginning of the 23S rRNA gene started with adenine instead of guanine (5'–AGTCAAGHKAATAAG–3').

Bayesian Inference and Maximum Parsimony analyses of the ITS regions recovered from three distinct operons gave internally consistent results (Fig. 8). Unlike the 16S rRNA analyses, *Trichotorquatus andrei* and *T. ladouxae* were clearly separated based on alignments of all three operons (Table 1). *T. maritimus, T. coquimbo*, and *Trichotorquatus* sp. 5 were distinct in all three phylogenies as well (Fig. 8).

The secondary structures of the conserved domains of the ITS regions were highly similar within species in the Type 1 and Type 2 operons (Figs. 5, 6), indicating that these operons likely share more recent common ancestry with each other than either does to the Type 3 operon, which had distinctly different structures (Figs. 5, 6). All five species which we recognize had differences in the D1-D1', Box-B, and V3 helices in all comparisons between orthologous operons.

DISCUSSION

Cryptogenera. In their discussion of what defines a cyanobacterial genus under modern criteria, Komárek et al. (2014) gave three criteria: (1) a unique supported phylogenetic position with a clear discontinuity (about 95% or less similarity) from the nearest sister clade; (2) distinct morphological separation from the nearest generic entities; and (3) related ecological niches for species in the genus. Based on phylogenetic analysis, the sister taxon to *Trichotorquatus* is *Kaipairowitsia,* which is ≤92.2% similar to *Trichotorquatus*, differs morphologically based on the filaments of *Kaipairowitsia* containing one to several trichomes in a common sheath, being

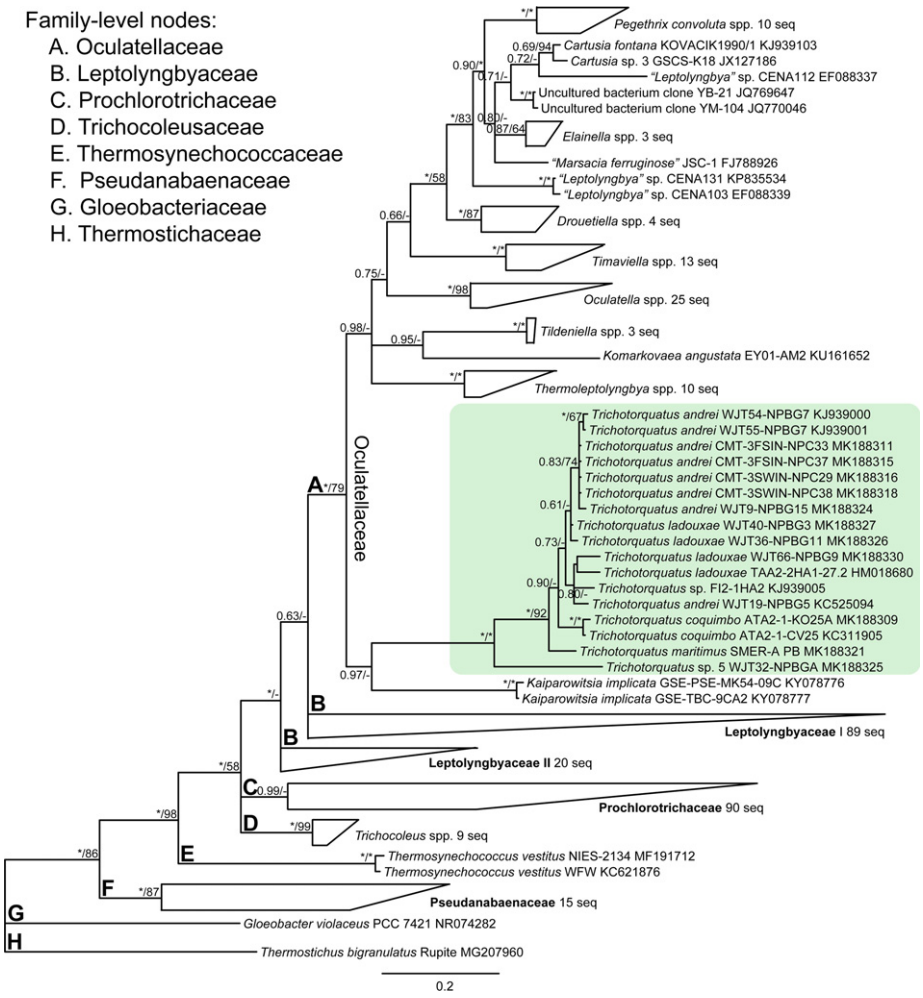

FIG. 7. Bayesian Inference analysis based on 329 sequences from families with simple filamentous or unicellular bacilloid taxa, with posterior probabilities and ML bootstrap values on nodes. Family-level nodes labeled with letter codes A-H are explained in list at upper left. Note, in this analysis Leptolyngbyaceae was not monophyletic. Family-level hierarchy follows recent publications (Komárek et al. 2014, 2020, Mai et al. 2018). [Colour figure can be viewed at wileyonlinelibrary.com]

unbranched, not having the collared sheath, forming nodules, and not having been shown to produce hormogonia or necridia in culture. *Kaipairowitsia* was isolated from a desert seep wall, which is also an ecological niche different than dryland soil. Consequently, *Trichotorquatus* meets all criteria of separation from its sister genus, validating the need to recognize it as a unique genus. All other genera in the Oculatellaceae were ≤92.5% similarity when compared to *Trichotorquatus*, further establishing its generic identity in the family (Table S3). All *Trichotorquatus* species were ≥94.5% similar (Table 1), consistent with microbiological standards for including species in the same genus (Yarza et al. 2014).

However, *Trichotorquatus* is not morphologically well-separated from *Leptolyngbya* sensu stricto, which, based on the type species *L. boryana* and related taxa (*L. foveolarum, L. angustata, L. corticola*), has thin trichomes (<4 μm wide), only one trichome per filament, false branching, and the ability to produce necridia. The only morphological feature separating *Trichotorquatus* (in the Oculatellaceae) from *Leptolyngbya* (Leptolyngbyaceae) is the telescoping sheath in *Trichotorquatus*. It is well established that sheath characteristics in the cyanobacteria are fairly unstable, and thus differences in sheath morphology are somewhat unsatisfactory for definition of genera. Such a high similarity in trait characteristics may lead to a high degree of confusion if cyanobacterial identification and classification is solely based on morphological characters.

Komárek et al. (2014) discuss the possibility that cryptic genera, or cryptogenera, might exist in cyanobacteria, and defined such taxa as genera that are phylogenetically distinct but morphologically indistinct. At the time, they did not know of any clear examples. *Trichotorquatus* is a clear example of a cryptic genus, having the primary morphological synapomorphies of *Leptolyngbya* sensu stricto (false

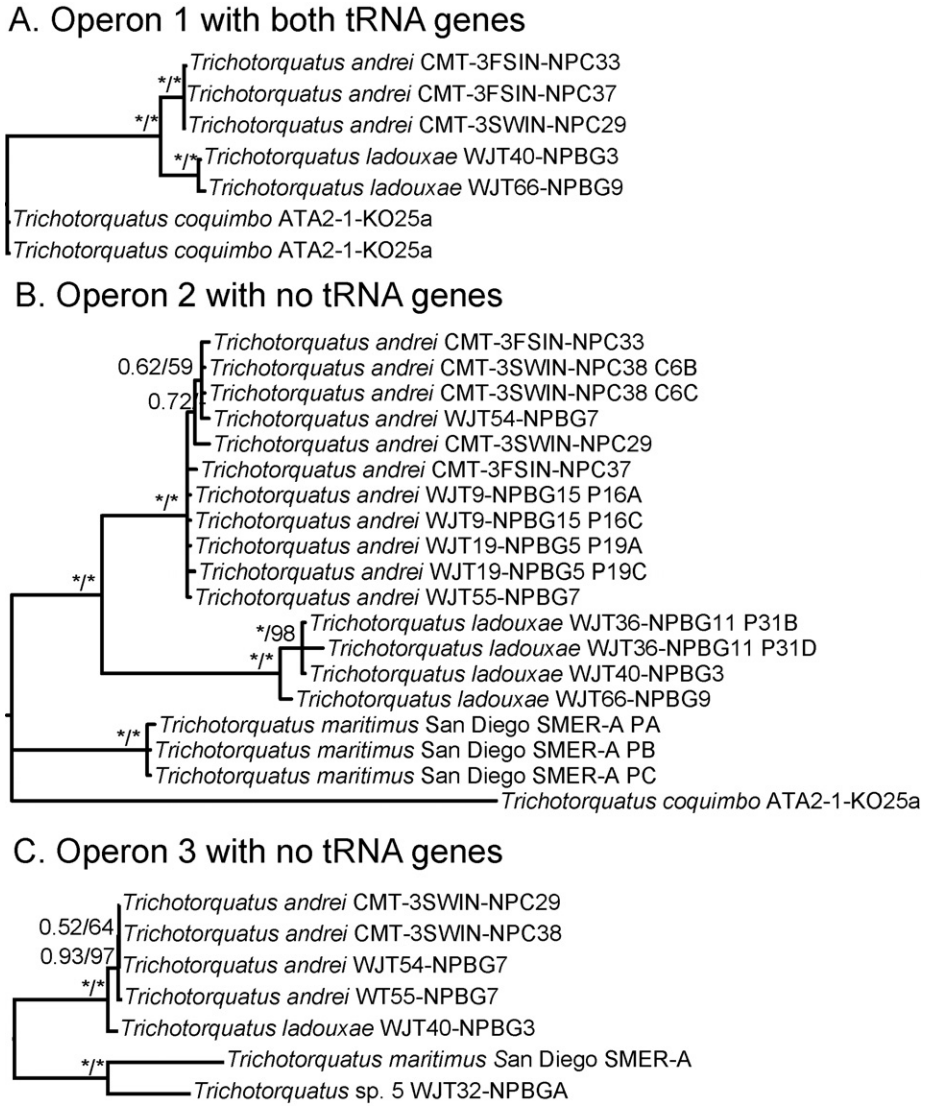

FIG. 8. Bayesian Inference analysis of 16S-23S ITS sequences, grouped by orthologous operons, with posterior probabilities and MP bootstrap values on nodes.

branching, necridia, single trichome per sheath). While some ecological separation exists (*Leptolyngbya* are often aerophytic, but typically from more mesic sites or even aquatic), the separation is not diagnostic. We anticipate that many more cryptogenera will likely be recognized in the Synechococcales and other cyanobacterial orders. There are already some genera that could arguably be considered cryptic genera in their segregation from *Nostoc*, such as *Mojavia, Halotia, Aliinostoc*, *Komarekiella, Desikacharya, Compactonostoc, Minunostoc,* and *Violetonostoc* (Řeháková et al. 2007, Genuário et al. 2015, Bagchi et al. 2017, Hentschke et al. 2017, Saraf et al. 2018, 2019, Cai and Li 2019, Cai et al. 2019a, b, 2020).

That this cryptic genus pair are found in two separate families is additionally problematic, as it means that Leptolyngbyaceae and Oculatellaceae cannot be recognized on morphological grounds, a conclusion which Mai et al. (2018) also reached when they described the Oculatellaceae. They proposed molecular means for separating the two families based on consistent sequence differences in five helices of the 16S rRNA gene (helices 18, 20, 23, 27, and 34). We checked these helices in *Trichotorquatus*, and the strains had the signature sequences for the family in all five helices, supporting the continued recognition of the families based on these molecular criteria. We suspect that when the revision of cyanobacteria is further along that many of the families will be defined by molecular criteria alone.

Species evaluation. All five species are well defined based on molecular criteria. They are all below the current species threshold of 98.7% for 16S rRNA comparisons (Table S3; see Yarza et al. 2014 for discussion of this threshold). Furthermore, in

TABLE 1. Percent dissimilarity among ITS regions in comparisons with orthologous operons. Comparisons among strains in the same species are reported in bold font, although in some instances multiple sequences were not available within species and this comparison cannot be reported According to recent standards, members of the same species generally have percent dissimilarities <3%, while percent dissimilarities >4% generally indicate that strains belong to different species.

OPERON 1				
	T. coquimbo	*T. andrei*	*T. ladouxae*	
T. coquimbo	**0.51%**			
T. andrei	16.11–16.50%	**0.18–0.53%**		
T. ladouxae	17.90–18.45%	7.12–8.16%	**1.01%**	
OPERON 2				
	T. maritimus	*T. coquimbo*	*T. andrei*	*T. ladouxae*
T. maritimus	**0.0–0.22%**			
T. coquimbo	16.44–16.67%	**N.A**		
T. andrei	11.41–12.32%	19.56–20.23%	**0.00–1.32%**	
T. ladouxae	13.36–14.47%	23.57–24.63%	10.48–13.12%	**0.00–2.00%**
OPERON 3				
	T. maritimus	*T. andrei*	*T. ladouxae*	*Tricho.* sp. 5
T. maritimus	**N.A.**			
T. andrei	27.70–28.22%	**0.00–1.72%**		
T. ladouxae	28.41%	5.83–6.69%	**N.A.**	
Trichotorquatus sp. 5	29.10%	25.68–26.21%	26.59%	**N.A.**

comparisons among orthologous operons, all five species have 16S-23S ITS dissimilarities ≥5.8 in all instances (Table 1), and most are ≥7.0, which is considered strong evidence for lineage separation worthy of taxonomic recognition (Osorio-Santos et al. 2014, Pietrasiak et al. 2014, 2019).

However, the species of *Trichotorquatus* are difficult to separate based on morphology alone. The most distinctive of the four species described herein is the type species, *T. maritimus*, which has wider trichomes and more robust, firm, widened sheaths than any of the other species. While the other three species differed statistically in their cell measurements, the degree of overlap in dimensions would make it nearly impossible to separate them based on morphological criteria, and consequently these are cryptic species. There is both molecular and biogeographic separation between *T. coquimbo* from South America and *T. andrei* and *T. ladouxae* from North America, so while morphologically cryptic, it would still be fairly easy to separate *T. coquimbo* from all North American taxa.

Trichotorquatus andrei and *T. ladouxae* are more problematic as they are sympatric species that are morphologically cryptic. Furthermore, the phylogenetic analysis based on 16S rRNA data did not succeed in clearly separating the two taxa (Fig. 7). Consequently, further evidence of their lineage separation is necessary in order to justify their taxonomic recognition. This evidence is found in the analysis of the 16S-23S ITS regions of the three ribosomal operons present in this genus. In phylogenetic analysis of the 16S-23S ITS, *T. andrei* and *T. ladouxae* were unambiguously separated on supported nodes (Fig. 8) in all three operons. Operon 2 was the most widely recovered ribosomal operon in *Trichotorquatus*, with eight strains of *T. andrei* and four strains of *T. ladouxae*. The fact that so many strains could be compared lends much greater credibility to claiming that they are phylogenetically distinct. Dissimilarity among the ITS regions of orthologous operons was >7.0% for operon 1, >10% for operon 2, and >5.5% for operon 3 (Table 1) dissimilarities indicative that they are separate species. The D1-D1' helix in operons 1 and 2 were notably different in secondary structure, as were the Box-B helices for the same operons (Fig. 7). Minor differences in the V3 helix of operons 1 and 2 existed mid-helix (Fig. 8). In operon 3, the D1-D1' and Box-B helices were identical in structure between the two species, but minor differences in structure could be seen in the V3 helix of this operon (Figs. 7, 8).

This study demonstrates the importance and robustness of sequencing multiple ribosomal operons for species-level determinations. If we had recovered only one operon in each strain, we may have incorrectly recognized more species based on differences that were due to paralogous operon differences rather than differences due only to comparisons within orthologous operons. Taxonomists and reviewers of taxonomic papers describing multiple cyanobacterial species based on ITS criteria need to be careful to avoid proliferation of species based on incomplete molecular characterizations. It was also helpful in this study to have multiple strains in the genus so that species-level patterns were clear.

In their description of *Myxacorys californica*, Pietrasiak et al. (2019) found evidence that speciation may be occurring in sympatric populations present in different microhabitats in desert soils, and Osorio-Santos et al. (2014) found that *Oculatella coburnii* and *O. mojaviensis*, though both occurring in the Mojave Desert, showed habitat separation based on soil parent materials. *Oculatella coburnii* grew on soils

derived from granite, while *O. mojaviensis* grew on soils derived from dolomite. Comparing the habitat descriptions for all of the strains identified as *Trichotorquatus andrei* and *T. ladouxae,* we did notice a pattern in ecological preferences between the two species (Table S1). *Trichotorquatus ladouxae* was found in sites WJT36, 40, and 66 that were characterized by having exclusively monzogranite as parent material. In contrast, all locations where *T. andrei* strains were collected were either non-granitic (dolomite for CMT strains, quartzite for WJT54) or had mixed sources of parent material (WJT9, 19, 55). A future population genetics study may be warranted investigating what delimits the range of each of our cryptic *Trichotorquatus* species.

A continuous need for taxonomic studies. Efforts in α–level taxonomy are critical to illuminate cyanobacterial diversity and provide us with insights into the evolutionary history and ecological significance of the diverse lineages we discover. Cyanobacterial taxonomy is in a state of great flux presently, with many new species and genera established recently. Advances are notably driven forward by the widespread adoption of a polyphasic approach that generally includes DNA-based characterization of the taxa under investigation. Associating a taxonomic ID and classification to genetic and/or genomic data then allows for the establishment of DNA-based phylogenetic benchmarks, leading to numerous improvements in data quality and quantity in microbial ecology and evolutionary biology.

As an example, linking taxonomic progress to DNA-based information is urgently needed to inform next-generation (short: next gen) sequencing efforts when surveying microbial communities across the globe. Next-gen sequencing surveys of soil habitats often reveal hundreds to thousands of unassigned sequences. Within cyanobacteria many undescribed or polyphyletic taxa are typically discovered (Garcia-Pichel et al. 2001, Patzelt et al. 2014, Hagemann et al. 2015, Williams et al. 2016, Becerra-Absalón et al. 2019, Muñoz-Martín et al. 2019). Almost as soon as a formal taxonomic description for a new taxon is complete and sequences are added to public sequence databases, records appear in subsequent next-gen studies as seen for *Trichocoleus*, *Chroakolemma*, and *Oculatella* (Dojani et al. 2013, Hagemann et al. 2015, Becerra-Absalón et al. 2019). We foresee a similar scenario happening for *Trichotorquatus*.

In summary, new taxonomic studies similar to our present paper will enable increasingly improved soil microbiome profiles to be documented, and thus our ecological inferences will become more meaningful. Advancing our understanding of algal biodiversity through continued efforts in taxonomy, while enriching the records of dryland soil cyanobacteria using next-gen sequencing surveys, may soon provide us with answers to the open questions of niche separation and population isolation in cyanobacteria. As we come to decipher diversity patterns and understand the finer scale ecology and niche preferences of cyanobacteria in soils, we will better be able to utilize cyanobacteria as indicators of environmental health and change (Muñoz-Martín et al. 2019).

We are grateful to the National Park Service for permission to work within Joshua Tree National Park and Mojave National Preserve. Sampling efforts in Joshua Tree National Park and Mojave National Preserve were supported by the California Desert Research Fund at The Community Foundation, Robert Lee Graduate Student Research Grant, and the Phycological Society Grants in Aid of Research fund awarded to Nicole Pietrasiak during her Ph.D. graduate program. Sample collection of soil from the Atacama Desert, isolation of ATA strains, and sequencing of those strains was completed with support from National Science Foundation grant number DEB–0842702. Any opinions, findings, conclusions, or recommendations expressed in this material are those of the authors and do not necessarily reflect the views of the National Science Foundation. Christina Vaccarino (one ATA strain) and Hend Alwathnani (TAA, FI strains) helped with strain isolation efforts. Paul De Ley offered insightful first reviews of the discussion before manuscript submission. The authors declare no conflict of interest. We thank the reviewers for their helpful comments.

Alwathnani, H. & Johansen, J. R. 2011. Cyanobacteria in soils from a Mojave Desert ecosystem. *Monogr. West. N. Am. Nat.* 5:71–89.

Bagchi, S. N., Dubey, N. & Singh, P. 2017. Phylogenetically distant clade of *Nostoc*-like taxa with the description of *Aliinostoc* gen. nov. and *Aliinostoc morphoplasticum* sp. nov. *Int. J. Syst. Evol. Micr.* 67:3329–38.

Becerra-Absalón, I., Johansen, J. R., Muñoz-Martín, M. A. & Montejano, G. 2018. *Chroakolemma* gen. nov. (Leptolyngbyaceae, Cyanobacteria) from soil biocrusts in the semi-desert Central Region of Mexico. *Phytotaxa* 367:201–18.

Becerra-Absalón, I., Johansen, J. R., Osorio-Santos, K. & Montejano, G. 2020. Two new *Oculatella* (Oculatellaceae, Cyanobacteria) species in soil crusts from tropical semi–arid uplands of México. *Fottea* 20:160–70.

Becerra-Absalón, I., Muñoz-Martín, M. A., Montejano, G. & Mateo, P. 2019. Differences in the cyanobacterial community composition of biocrusts from the drylands of Central Mexico. Are there endemic species? *Front. Microbiol.* 10:937.

Belnap, J., Büdel, B. & Lange, O. L. 2003. Biological soil crusts: Characteristics and distribution. *In* Belnap, J. & Lange, O. L. [Eds.] *Ecological Studies 150.* Springer-Verlag, Berlin Heidelberg, pp. 3–30.

Bohunická, M., Pietrasiak, N., Johansen, J. R., Berrendero-Gomez, E., Hauer, T., Gaysina, L. & Lukešová, A. 2015. *Roholtiella*, gen. nov. (Nostocales, Cyanobacteria) – a tapering and branching member of the Nostocaceae (Cyanobacteria). *Phytotaxa* 197:84–103.

Boyer, S. L., Flechtner, V. R. & Johansen, J. R. 2001. Is the 16S–23S rRNA internal transcribed spacer region a good tool for use in molecular systematics and population genetics? A case study in cyanobacteria. *Mol. Biol. Evol.* 18:1057–69.

Boyer, S. L., Johansen, J. R., Flechtner, V. R. & Howard, G. L. 2002. Phylogeny and genetic variance in terrestrial *Microcoleus* (Cyanophyceae) species based on sequence analysis of the 16S rRNA gene and associated 16S–23S ITS region. *J. Phycol.* 38:1222–35.

Büdel, B., Dulić, T., Darienko, T., Rybalka, N. & Friedl, T. 2016. Cyanobacteria and algae of biological soil crusts. *In* Weber, B., Büdel, B. & Belnap, J. [Eds.] *Ecological Studies.* Springer International Publishing, Champaign, pp. 55–80.

Burke, D. J., Kretzer, A. M., Rygiewicz, P. T. & Topa, A. M. 2006. Soil bacterial diversity in a loblolly pine plantation: influence of ectomycorrhizas and fertilization. *FEMS Microbiol. Ecol.* 57:409–19.

Cai, F., Li, X., Geng, R., Peng, X. & Li, R. 2019a. Phylogenetically distant clade of *Nostoc*-like taxa with the description of *Minunostoc* gen. nov. and *Minunostoc cylindricum* sp. nov. *Fottea* 19:13–24.

Cai, F., Li, X., Yang, Y., Jia, N., Huo, D. & Li, R. 2019b. *Compactonostoc shennongjiaensis* gen. & sp. nov. (Nostocales, Cyanobacteria) from a wet rocky wall in China. *Phycologia* 58:200–10.

Cai, F. & Li, R. 2019. Validation of *Compactonostoc shennongjiaense* gen. et sp. nov. (Nostocaceae, Cyanobacteria). *Notulae Algarum* 121:1.

Cai, F., Peng, X. & Li, R. 2020. *Violetonostoc minutum* gen et sp. nov. (Nostocales, Cyanobacteria) from a rocky substrate in China. *Algae Int. J. Algal Res.* 35:1–15.

Carmichael, W. W. 1986. Isolation, culture, and toxicity testing of toxic freshwater cyanobacteria (blue-green algae). *In* Shilov, V. [Ed.] *Fundamental research in homogenous catalysis.* Vol. 3. Gordon and Breach, New York, pp. 1249–62.

Casamatta, D. A., Johansen, J. R., Vis, M. L. & Broadwater, S. T. 2005. Molecular and morphological characterization of ten polar and near-polar strains within the Oscillatoriales (Cyanobacteria). *J. Phycol.* 41:421–38.

Darriba, D., Taboada, G. L., Doallo, R. & Posada, D. 2012. jModelTest2: More models, new heuristics and parallel computing. *Nat. Methods* 9:772.

Dodds, W. K., Gudder, D. A. & Mollenhauer, D. 1995. The ecology of *Nostoc*. *J. Phycol.* 31:2–18.

Dojani, S., Kauff, F., Weber, B. & Büdel, B. 2013. Genotypic and phenotypic diversity of Cyanobacteria in biological soil crusts of the succulent Karoo and Nama Karoo of Southern Africa. *Microb. Ecol.* 67:286–301.

Elbert, W., Weber, B., Burrows, S., Steinkamp, J., Büdel, B., Andreae, M. O. & Pöschl, U. 2012. Contribution of cryptogamic covers to the global cycles of carbon and nitrogen. *Nature Geosci.* 5:459–62.

Evans, R. D. & Johansen, J. R. 1999. Microbiotic crusts and ecosystem processes. *Critical Rev. Plant Sci.* 18:183–225.

Flechtner, V. R., Boyer, S. L., Johansen, J. R. & DeNoble, M. L. 2002. *Spirirestis rafaelensis* gen. et sp. nov. (Cyanophyceae), a new cyanobacterial genus from desert soils. *Nova Hedwigia* 74:1–24.

Flechtner, V. R., Johansen, J. R. & Belnap, J. 2008. The biological soil crusts of the San Nicolas Island: enigmatic algae from a geographically isolated system. *West. N. Am. Nat.* 68:405–36.

Garcia-Pichel, F., López-Cortés, A. & Nübel, U. 2001. Phylogenetic and morphological diversity of cyanobacteria in soil desert crusts from the Colorado Plateau. *Appl. Environ. Microbiol.* 67:1902–10.

Genuário, D. B., Vieira Vaz, M. G. M., Hentschke, G. S., Sant'Anna, C. L. & Fiore, M. F. 2015. *Halotia* gen. nov., a phylogenetically and physiologically coherent cyanobacterial genus isolated from marine coastal environments. *Int. J. Syst. Evol. Microbiol.* 65:663–675.

Giraldo-Silva, A., Nelson, C., Barger, N. N. & Garcia-Pichel, F. 2019. Nursing biocrusts: isolation, cultivation, and fitness test of indigenous cyanobacteria. *Restor. Ecol.* 27:793–803.

Hagemann, M., Henneberg, M., Felde, V. J., Drahorad, S. L., Berkowicz, S. M., Felix-Henningsen, P. & Kaplan, A. 2015. Cyanobacterial diversity in biological soil crusts along a precipitation gradient, Northwest Negev Desert, Israel. *Microb. Ecol.* 70:219–30.

Hentschke, G. S., Johansen, J. R., Pietrasiak, N., Rigonato, J., Fiore, M. F. & Sant'Anna, C. L. 2017. *Komarekiella atlantica* gen. et sp. nov. (Nostocaceae, Cyanobacteria): a new subaerial taxon from the Atlantic Rainforest and Kauai, Hawaii. *Fottea, Olomouc* 17:178–90.

Johansen, J. R. 1993. Cryptogamic crusts of semiarid and arid lands of North America: Minireview. *J. Phycol.* 29:140–7.

Johansen, J. R. & Shubert, L. E. 2001. Algae in soils. *Nova Hedwigia, Beiheft* 123:297–306.

Johansen, J. R., Olsen, C. E., Lowe, R. L., Fučiková, K. & Casamatta, D. A. 2008. *Leptolyngbya* species from selected seep walls in the Great Smoky Mountains National Park. *Algol. Stud.* 126:21–36.

Johansen, J. R., Kovacik, L., Casamatta, D. A., Fučiková, K. & Kaštovský, J. 2011. Utility of 16S–23S ITS sequence and secondary structure for recognition of intrageneric and intergeneric limits within cyanobacterial taxa: *Leptolyngbya corticola* sp. nov. (Pseudanabaenaceae, Cyanobacteria). *Nova Hedwigia* 92:283–302.

Komárek, J. & Anagnostidis, K. 2005. *Cyanoprokaryota – 2nd Part: Oscillatoriales.* Elsevier/Spektrum, Heidelberg, 759 pp.

Komárek, J., Kaštovsky, J., Mareš, J. & Johansen, J. R. 2014. Taxonomic classification of cyanoprokaryotes (cyanobacterial genera) according to the polyphasic approach. *Preslia* 86: 295–335.

Komárek, J., Johansen, J. R., Šmarda, J. & Strunecký, O. 2020. Phylogeny and taxonomy of *Synechococcus*–like cyanobacteria. *Fottea* 20:171–91.

Larkin, M. A., Blackshields, G., Brown, N. P., Chenna, R., McGettigan, P. A., McWilliam, H., Valentin, F., Wallace, I. M., Wilm, A., Lopez, R., Thompson, J. D., Gibson, T. J. & Higgins, D. G. 2007. ClustalW and ClustalX version 2. *Bioinformatics* 23:2947–8.

Mai, T., Johansen, J. R., Pietrasiak, N., Bohunická, M. & Martin, M. P. 2018. Revision of the Synechococcales (Cyanobacteria) through recognition of four families including Oculatellaceae fam. nov. and Trichocoleaceae fam. nov. and six new genera containing 14 species. *Phytotaxa* 325:1–59.

Maier, S., Tamm, A., Wu, D., Caesar, J., Grube, M. & Weber, B. 2018. Photoautotrophic organisms control microbial abundance, diversity, and physiology in different types of biological soil crusts. *ISME J.* 12:1032–46.

Mareš, J., Johansen, J. R., Hauer, T., Zima, J. Jr, Ventura, S., Cuzman, O., Tiribilli, B. & Kaštovský, J. 2019. Taxonomic resolution of the genus *Cyanothece* (Chroococcales, Cyanobacteria), with a treatment on *Gloeothece* and three new genera, *Crocosphaera*, *Rippkaea*, and *Zehria*. *J. Phycol.* 55:578–610.

Mesfin, M., Johansen, J. R., Pietrasiak, N. & Balderelli, L. M. 2020. *Nostoc oromo* sp. nov. (Nostocales, Cyanophyceae) from Ethiopia: a new species based on morphological and molecular evidence. *Phytotaxa* 433:81–93.

Miller, M., Schwartz, T., Pickett, B., He, S., Klem, E., Scheuermann, R. H., Passarotti, M., Kaufman, S. & O'Leary, M. A. 2015. A RESTful API for Access to Phylogenetic Tools via the CIPRES Science Gateway. *Evol. Bioinform.* 11:43–8.

Mühlsteinová, R., Johansen, J. R., Pietrasiak, N., Martin, M. P., Osorio-Santos, K. & Warren, S. D. 2014a. Polyphasic characterization of *Trichocoleus desertorum* sp. nov. (Pseudanabaenales, Cyanobacteria) from desert soils and phylogenetic placement of the genus *Trichocoleus*. *Phytotaxa* 193:241–61.

Mühlsteinová, R., Johansen, J. R., Pietrasiak, N. & Martin, M. P. 2014b. Polyphasic characterization of *Kastovskya adunca* gen. nov. et comb. nov. (Oscillatoriales, Cyanobacteria) from desert soils of the Atacama Desert, Chile. *Phytotaxa* 163:216–28.

Muñoz-Martín, M. Á., Becerra-Absalón, I., Perona, E., Fernández-Valbuena, L., Garcia-Pichel, F. & Mateo, P. 2019. Cyanobacterial biocrust diversity in Mediterranean ecosystems along a latitudinal and climatic gradient. *New Phytol.* 221:123–41.

Nübel, U., Garcia-Pichel, F. & Muyzer, G. 1997. PCR primers to amplify 16S rRNA genes from cyanobacteria. *Appl. Environ. Microbiol.* 63:3327–32.

Osorio-Santos, K., Pietrasiak, N., Bohunická, M., Miscoe, L. H., Kováčik, L., Martin, M. P. & Johansen, J. R. 2014. Seven new species of *Oculatella* (Pseudanabaenales, Cyanobacteria). *Eur. J. Phycol.* 49:450–70.

Patzelt, D. J., Hodač, L., Friedl, T., Pietrasiak, N. & Johansen, J. R. 2014. Biodiversity of soil cyanobacteria in the hyper-arid Atacama Desert, Chile, assessed by culture dependent and independent approaches. *J. Phycol.* 50:698–710.

Perkerson, R., Johansen, J. R., Kovacik, L., Brand, J. & Casamatta, D. A. 2011. A unique Pseudanbaenalean (Cyanobacteria) genus *Nodosilinea* gen. nov. based on morphological and molecular data. *J. Phycol.* 47:1397–412.

Pietrasiak, N., Mühlsteinová, R., Siegesmund, M. & Johansen, J. R. 2014. Phylogenetic placement of *Symplocastrum* (Phormidiaceae, Cyanobacteria) with descriptions of two new species: *S. flechtnerae* and *S. torsivum*. *Phycologia* 53:529–41.

Pietrasiak, N., Osorio-Santos, K., Shalygin, S., Martin, M. P. & Johansen, J. R. 2019. When is a lineage a species? A case study in *Myxacorys* gen. nov. (Synechococcales: Cyanobacteria) with the description of two new species from the Americas. *J. Phycol.* 55:976–96.

Rambaut, A. 2018. FigTree v1.4.4, A Graphical Viewer of Phylogenetic Trees. Available from http://tree.bio.ed.ac.uk/software/figtree/.

Řeháková, K., Johansen, J. R., Casamatta, D. A., Xuesong, L. & Vincent, J. 2007. Morphological and molecular characterization of selected desert soil cyanobacteria: three species new to science including *Mojavia pulchra* gen. et sp. nov. *Phycologia* 46:481–502.

Rivera-Aguilar, V., Montejano, G., Rodríguez-Zaragoza, S. & Durán-Díaz, A. 2006. Distribution and composition of cyanobacteria, mosses and lichens of the biological soil crusts of the Tehuacán Valley, Puebla, México. *J. Arid Environ.* 67:208–25.

Saraf, A. G., Dawda, H. G. & Singh, P. 2018. *Desikacharya* gen. nov., a phylogenetically distinct genus of Cyanobacteria along with the description of two new species, *Desikacharya nostocoides* sp. nov. and *Desikacharya soli* sp. nov., and reclassification of *Nostoc thermotolerans* to *Desikacharya thermotolerans* comb. nov. *Int. J. Syst. Evol. Microbiol.* 69:307–15.

Saraf, A. G., Dawda, H. G. & Singh, P. 2019. Validation of the genus *Desikacharya* gen. nov. (Nostocaceae, Cyanobacteria) and three included species. *Notulae Algarum* 107:1–3.

Shalygin, S., Shalygina, R., Redkina, V. V., Gargas, C. B. & Johansen, J. R. 2020. Description of *Stenomitos kolaenensis* and *S. hiloensis* sp. nov. (Leptolyngbyaceae, Cyanobacteria) with an emendation of the genus. *Phytotaxa* 440:108–28.

Swofford, D. L. 1998. *PAUP*: Phylogenetic analysis using parsimony (and other methods)*. Sinauer Associates, Sunderland, Massachusetts.

Taton, A., Grubisic, S., Ertz, D., Hodgson, D. A., Piccardi, R., Biondi, N., Tredici, M. R., Mainini, M., Losi, D., Marinelli, F. & Wilmotte, A. 2006. Polyphasic study of Antarctic cyanobacterial strains. *J. Phycol.* 42:1257–70.

Thiers, B. 2020. Index Herbariorum: A Global Directory of Public Herbaria and Associated Staff. New York Botanical Garden's Virtual Herbarium. http://sweetgum.nybg.org/science/ih [accessed 11 June 2019].

Turland, N. J., Wiersema, J. H., Barrie, F. R., Greuter, W., Hawksworth, D. L., Herendeen, P. S. & Knapp, S., et al. [Eds.] 2018. *International Code of Nomenclature for algae, fungi, and plants (Shenzhen Code) adopted by the Nineteenth International Botanical Congress Shenzhen, China, July 2017. Regnum Vegetabile 159*. Koeltz Botanical Books, Glashütten.

Turner, S. 1997. Molecular systematics of the oxygenic photosynthetic bacteria. *Pl. Syst. Evol.* 11:13–52.

Vaz, M. G. M. V., Genuário, D. B., Andreote, A. P. D., Malone, C. F. S., Sant'Anna, C. L., Barbiero, L. & Fiore, M. F. 2015. *Pantanalinema* gen. nov. and *Alkalinema* gen. nov.: novel pseudanabaenacean genera (Cyanobacteria) isolated from saline-alkaline lakes. *Int. J. Syst. Evol. Microbiol.* 65:298–308.

Williams, L., Loewen-Schneider, K., Maier, S. & Büdel, B. 2016. Cyanobacterial diversity of western European biological soil crusts along a latitudinal gradient. *FEMS Microbiol. Ecol.* 92: fiw157.

Wilmotte, A., Auwera, G. V. D. & Wachter, R. D. 1993. Structure of the 16S rRNA of the thermophilic cyanobacterium *Chlorogloeopsis* HTF ('*Mastigocladus laminosus* HTF') strain PCC7518, and phylogenetic analysis. *FEBS* 317:96–100.

Yarza, P., Yilmaz, P., Pruesse, E., Glöckner, F. O., Ludwig, W., Schleifer, K., Whitman, W. B., Euzéby, J., Amann, R. & Rosselló-Móra, R. 2014. Uniting the classification of cultured and uncultured bacteria and archaea using 16S rRNA gene sequences. *Nature Rev. Microbiol.* 12:635–45.

Yeager, C. M., Kuske, C. R., Carney, T. D., Johnson, S. L., Ticknor, L. O. & Belnap, J. 2012. Response of biological soil crust diazotrophs to season, altered summer precipitation, and year-round increased temperature in an arid grassland of the Colorado Plateau, USA. *Front. Microbiol.* 3:358.

Zuker, M. 2003. Mfold web server for nucleic acid folding and hybridization prediction. *Nuc. Acids Res.* 31:3406–15.

Supporting Information

Additional Supporting Information may be found in the online version of this article at the publisher's web site:

Figure S1. Uncollapsed Bayesian Inference Analysis showing all sequences used in construction of collapsed phylogeny shown in Figure 7, with A-H on nodes indicating family level clades.

Table S1. Meta-data associated with each *Trichotorquatus* strain evaluated in our study

Table S2. GenBank numbers associated with *Trichotorquatus* sequences used in this study.

Table S3. Percent similarity of members of Oculatellaceae based on 16S rRNA gene sequence.